Reconstructions of Pleistocene Glaciers in Rhoades Canyon and Lake Fork Valley in the Uinta Mountains, Utah, USA

By
Kathryn Lawson

Submitted senior thesis for required fulfillment for
Bachelor of Arts Degree
(Geology)
Gustavus Adolphus College
2006

Reconstructions of Pleistocene Glaciers in Rhoades Canyon and Lake Fork Valley in the Uinta Mountains, Utah, USA

By
Kathryn Lawson
Thesis advisor Professor Benjamin Laabs

ABSTRACT

Mountain glacial deposits in the Uinta Mountains provide a detailed record for exploring the history of glaciations in northern Utah. Glacial modeling of Rhodes Canyon and the Lake Fork Canyon can help explore the processes of glacial flow and can be used to infer paleoclimate within the Uinta Mountains. Moraines and topographic data were used for input to the glacier flow-line model. Ice extent and thickness extrapolations were used to test an ice cap theory for Rhodes Canyon. An ice cap would not only affect the glacial flow through Rhodes Canyon but also the flow into adjacent valleys. The extrapolated ice thickness at the peak of Rhodes Canyon is estimate at 100 to 160 meters of ice above the surface supporting the theory that an ice cap fed the Rhodes and Wolf Creek Canyon glaciers. A similar approach was used in the Lake Fork Canyon to estimate the ice flux and ablation gradient, ultimately aiding in understanding the paleoclimate for the Lake Fork. The diminutive ablation gradient of 0.35mm/m indicates a dry and frigid environment for glacial formation within the Lake Fork.

CONTENTS

Figure Index

Table Index

INTRODUCTION

Glacier reconstruction holds the key to understanding thousands of years of Earth's history. It not only explains the formation but also the location of glacial land features, and ultimately unlocks clues to the paleoclimate of post-glaciated regions. Glacier modeling is the basis for glacier reconstruction. Glacier reconstruction is helpful for understanding the ice dynamics and flow properties of glaciers such as basal shear stress and flow velocity. The flow properties of glaciers can ultimately help determine the environmental conditions during which the glacier formed.

My research consists of reconstructing glacial flow through Rhodes Canyon and the Lake Fork of the Uinta Mountains, Utah by applying a modified glacial flow-line model modified from Murray and Locke (1989). Glacial modeling of Rhodes Canyon and the Lake Fork described herein provides clues to glacial flow during the last Quaternary glaciation throughout the Uinta Mountains. The glacial reconstruction of Rhodes Canyon through the use of glacial modeling can determine the extrapolated ice thickness above the equilibrium line altitude (ELA). The correlation between ice thickness and topographic elevation will allow for the calculation of an ice cap, which would alter the flow and formation of glaciers in Rhodes Canyon, Soapstone Basin and the Wolf Creek (Figure 1).

Glacial modeling can calculate the glacial discharge, basal shear stress, and ablation gradient for post-glaciated valleys. Glacial reconstruction of the ablation zone using glacial landform data allows for a total area estimation of the valley. The ablation gradient is the change in net melting per unit elevation within the ablation zone of the glacier. The paleoclimate of the region can be determined by multiplying the melting rate by the ablation area versus the slope of the valley. This model was applied to the Lake Fork for interpretations of paleocliamte.

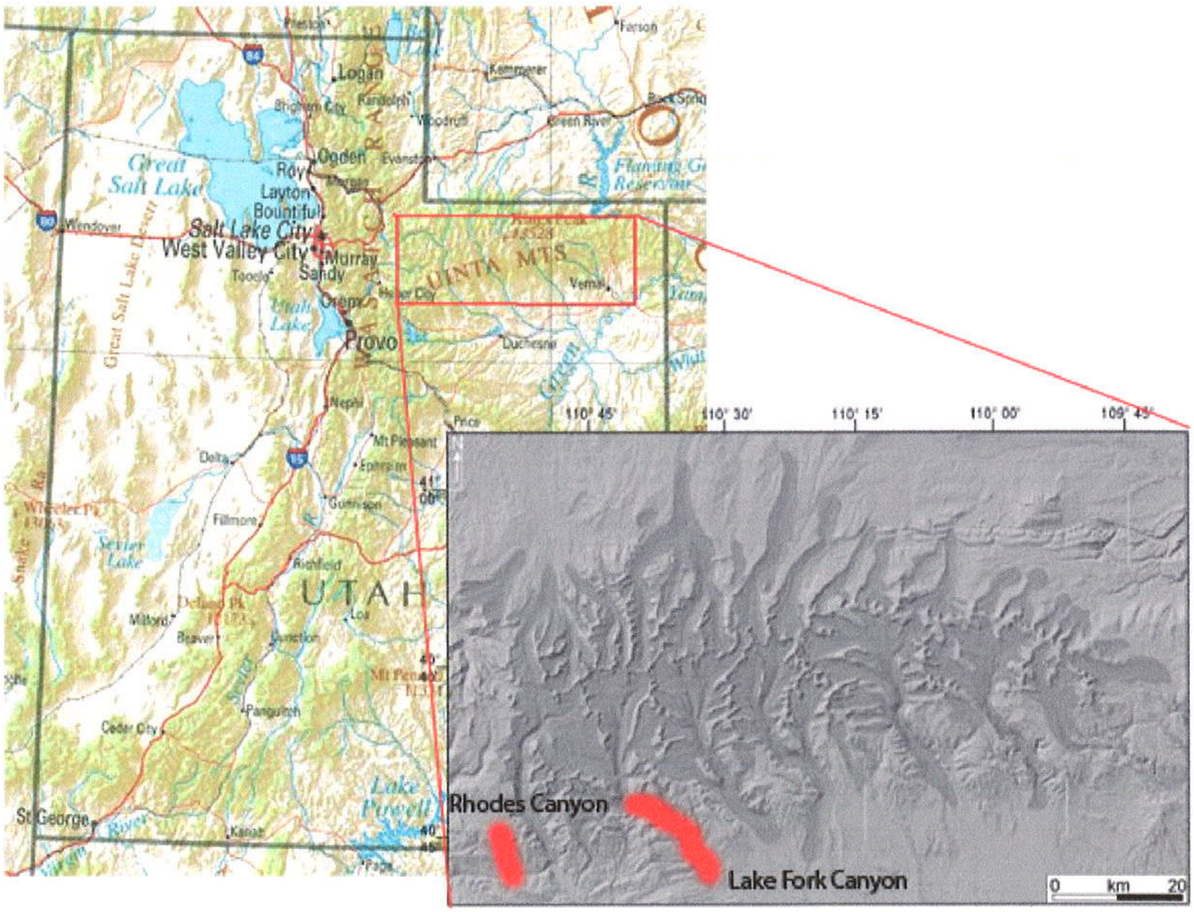

Figure 1. Topographic map of Utah with enlarged ice extent of the Uinta Mountains. Thodes Canyon and the Lake Fork Canyon marked with shading.

Uinta Mountains

The Uinta Mountains are located in the central Rocky Mountains within the Utah borders. The Uinta Mountains were uplifted during the Laramide Orogeny, in the late Mesozoic to the early Cenozoic Era. The deformation of the Uinta Mountains is distinguished by crustal shortening resulting in an east-west folding and faulting trend of both the north and south flanks. The Uinta Mountains has been divided into two main regions: the western glaciated region and the eastern non-glaciated region. The major drainage basins flow northward or southward away from the crest of the ridge. Most of the western drainage basins were eroded during glaciations.

The western side of the Uinta Mountains is considered to have been extensively more glaciated in comparison to the eastern side. This is depicted by the ELAs of the Smiths Fork Glaciation that decrease from west to east. The western Uinta Mountains were more glaciated because of their proximity to Lake Bonneville, resulting in pluvial conditions and an increase in precipitation due to lake effect moisture (Munroe and Mickelson 2002). The overall paleoclimate of the western region is considered to have been cold and wet. In contrast, the eastern side of the Uinta Mountains received less precipitation resulting in a drier climate. Isotope signatures give evidence for the precipitation differences between the east and west regions (Laabs 2004). The origin of precipitation can be determined by the weight difference between oxygen 16 and 18. Oxygen 18 has a greater weight than oxygen 16 resulting in its falling out of precipitation closer to the source. The high elevation of the western Uinta Mountains prevented the precipitation of oxygen 18 on the eastern side of the range. This resulted in a higher precipitation rate on the western side resulting in a cold and dry paleoclimate (Munroe and Mickelson 2002).

Three major glaciations occurred throughout the Rocky Mountains: the Sacagawea Ridge (659-620ka), the Bull Lake (186-128ka), and the Pinedale (24-12ka) (Laabs 2004). The correlated Uinta glaciations are Altonah, Blacks Fork and Smiths Fork respectively. This paper research of moraines in the Uinta Mountains focuses exclusively on the Smiths Fork-aged moraines that are the innermost terminal moraines in each valley.

Rhodes Canyon and Lake Fork Canyon

Rhodes Canyon is located on the west side of the Uinta Mountains adjacent to the Ashley National Forest (Figure 1). The lower portion of this post-glaciated valley is steep-sided and is defined by a distinct V-shape, which is not typical for glacial valleys (Figure 2B). At the base of Rhodes Canyon, the topography is extremely hummocky (Figure 3A) with partially exposed cherty limestone outcrops protruding from the valley walls. The lateral and terminal moraines along Rhodes Canyon are moderately preserved and only exist at the base of the valley or near the ELA. The till that comprises moraine ridges contains a mixture of boulders predominately of sandstone with occasionally occurring boulders of cherty limestone scoured from the bedrock outcrops farther up ice. The moraine crests on either side of the valley are scattered with a diamicton composition of pebble to cobble-sized rocks (Figure 3B). Rhodes Canyon is peculiar because of the large amount of ice that flowed through a very narrow and steeply dipping valley without significant erosion (Figure 2B).

The Lake Fork Canyon is located on the south side of the Uinta Mountains, Utah. The Lake Fork is divided by a bedrock knob, Round Mountain, which forced the Lake Fork River to flow along the east side of the valley (Laabs 2004). The Lake Fork Canyon's glacial characteristics are typical for post-glaciated valleys in the Uinta Mountains including well preserved lateral, recessional, and terminal moraines (Figure 2C). These Smiths Fork-age lateral moraines are well preserved on both sides of the valley and are distinguished from the Blacks Fork by their fresh appearance and a lower elevation.

Similar modeling techniques were applied to both the Lake Fork and Rhodes Canyon's different objectives. The model was used to predict the ice thickness at the top of Rhodes Canyon in attempts to explain the glacial landforms. The paleoclimate of the Lake Fork was calculated using the same model. Glacier modeling can be used in many ways to reconstruct glaciers and explain glacier features or interpret the paleo-environment.

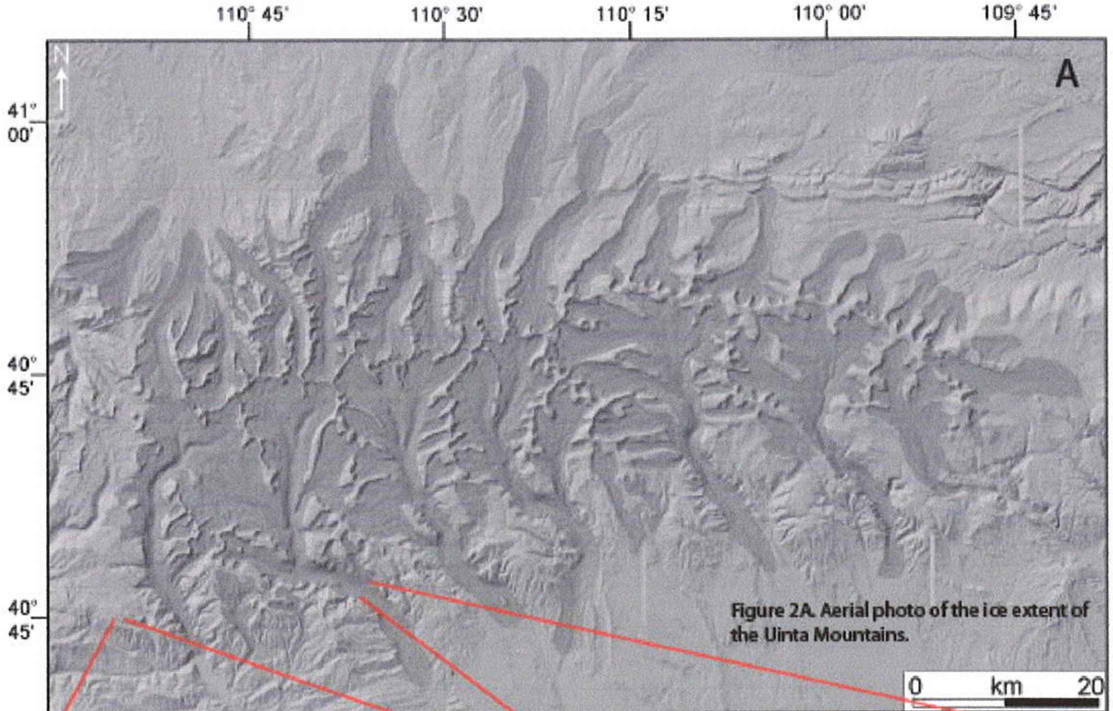

Figure 2A. Aerial photo of the ice extent of the Uinta Mountains.

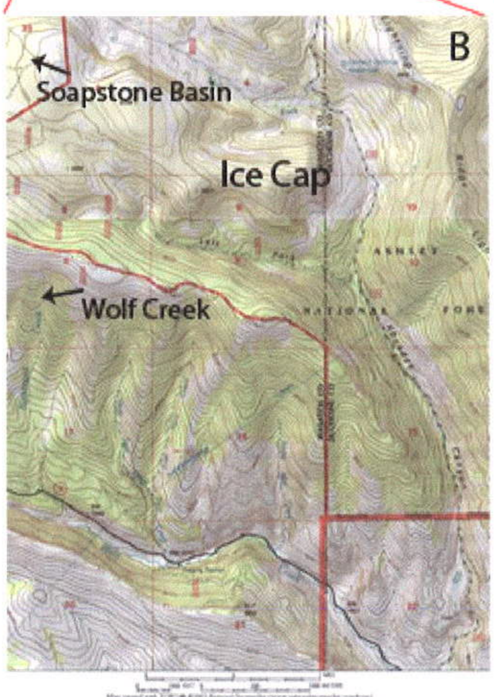

Figure 2B. Enlarged topographic map of Rhodes Canyon. Ice cap marked with flow directions into Soapstone Basin and the Wolf Creek.

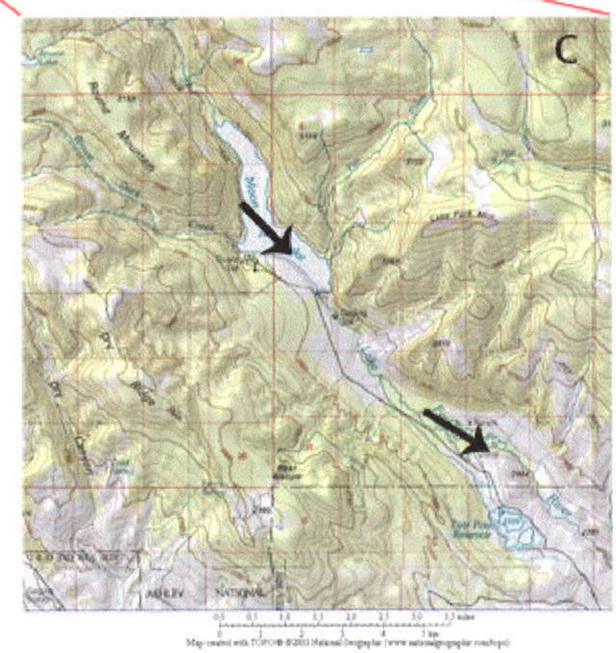

Figure 2C. Lake Fork Canyon showing glacial flow with arrows.

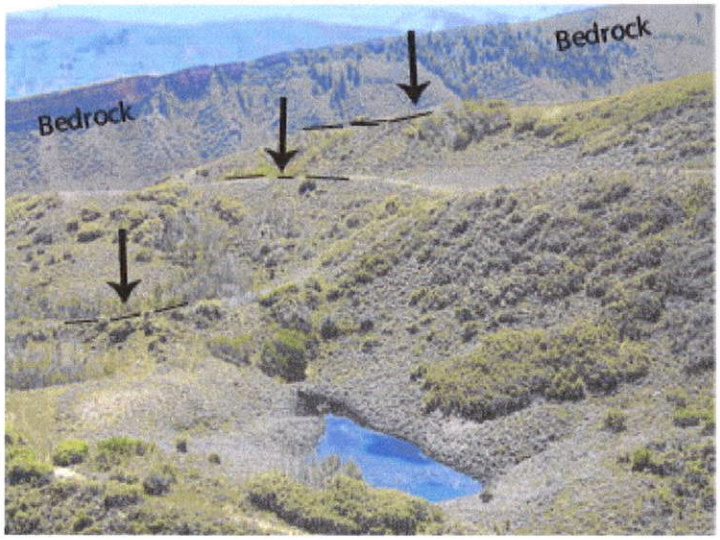

Figure 3A. Hummokcy topography at the base of Rhodes Canyon from the Pinedale aged Glaciation.

Figure 3B. Diamicton mix of pebble to cobbel sized rocks on the moraine crests throughout Rhodes Canyon.

Glacial Geology

By definition, a glacier occurs when the accumulation of snow, hail, frost, avalanched snow and rainfall exceeds the ablation rate of melting, calving or sublimination of snow and ice (Bennet and Glasser 1996). The glacier is forced into movement through the transfer of mass from the accumulation zone to the ablation zone. This imbalance of mass is due to gravitational forces acting on the glacier. The gravitational force alters the slope of the glacier and ultimately drives the direction and velocity of ice flow. This transformation can occur by compaction, expulsion of air, and the growth of ice crystals (Bennet and Glasser 1996) and consequently increases the surface slope and stress that is imposed on the ice.

The basal ice temperature, which controls the amount of melt water, is dependent upon the ice thickness, the accumulation rate, the ice surface temperature, geothermal heat and frictional heat (Bennet and Glasser 1996). The amount of melt water directly influences the glacier's velocity and rate of erosion. An increase in ice thickness results in an increase in basal shear stress which increases the velocity and ultimately the rate of deformation.

Ice flow can occur in three different ways. The first method is by internal deformation of ice crystals resulting from the increase in the rate of creep which also increases with shear stress. Shear stress is the frictional force of the glacier on its bed and the deformation due to gravity. Basal sliding is another method of ice flow and is the sliding of the glacier over obstacles. The final method of ice flow is by subglacial bed deformation which occurs when an ice sheet flows over unfrozen material causing the sediment to deform (Bennet and Glasser 1996). The greatest velocity of ice flow occurs at the center of the valley because it is the farthest point from frictional resistance along the valley sides and is also where the ice is thickest. The velocity at which creep, always a contributing factor to glacial movement, moves can be predicted by using estimates of ice thickness, slope and shear stress.

Background

Professors J. Munroe and B. Laabs have collected information synonymous with my research, including field mapping, and dating glaciations throughout the Uinta Mountains (Munroe and Mickelson 2002, Laabs 2004). Their findings conclude that at least three glaciations occurred during the Quaternary Period for the Uinta Mountains: the Altonah, Blacks Fork, and Smiths Fork (Munroe and Mickelson 2002). The Lake Fork moraines have been dated at 19-16ka for the Smiths Fork and estimated as correlating with MIS 6 for Blacks Fork (Laabs 2004).

METHODS

Field Methods

Rhodes Canyon was mapped using field research and interpreted during the summer of 2005. The terminal, recessional, and lateral moraines were distinguished using field data, topographic maps, and moraine crest elevations which verified the glacial landforms age. Glacial evidence including boulder erratics and striations were recorded as further data concluding a post-glaciated valley for Rhodes Canyon.

Glacial Modeling

Murray and Locke (1989) used glacial reconstruction to model the Timber Glacier in Crazy Mountains, Montana. The glacial model was used to reconstruct the glacial profile and aereal extent of the valley. Using a basic equation the basal shear stress of the valley could be calculated and then averaged to find the center flow-line velocity. The center flow-line velocity can be deduced with the assumptions of zero basal sliding and a constant basal shear stress above the ELA. Finally, the estimation of mass balance from the calculated mass flux can be used to determine properties of the glacier and the paleoclimate of the region.

I inserted my data into their glacial model for its application to Rhodes Canyon and the Lake Fork. I initially reconstructed the glacial profile and aerial extent of the post-glaciated valley. The basal shear stress along the longitudinal profile was calculated next allowing for the deduction of flow rates and ultimately the estimation of the mass balance and the paleoclimate of the region. I took a slightly different approach for both Rhodes Canyon and the Lake Fork Canyon. By calculating each valley's flow dynamics I was able to determine if an ice cap affected flow through Rhodes Canyon and I was able to interpret the paleoclimate for the Lake Fork.

Rhodes Canyon

I used Murray and Locke's (1989) glacial modeling approach and applied a flow-line model to reconstruct post-glaciated valleys in the Uinta Mountains, Utah. I recorded the bedrock and moraine crest elevations continuously every 500 meters up valley using a 1:24000 scale map of Rhodes Canyon and then used these elevations to estimate the center flow line up to the ELA and reconstructed the ice extent (Appendix 1). The ELA, 2676 meters, was estimated to be equivalent to that in the Duchesne valley directly east of Rhodes Canyon (Laabs and Carson 2005). .

My glacial model used the basal shear stress (τ) to find the creep velocity at the equilibrium line of the glacier. The modeling approach I used assumed a constant ice density of 900kg/m^3 and pg, the ice density multiplied by gravity, is constant at 8820kg/m^3, t is the ice thickness at the center line of the valley, and α is the slope of the valley.

$$\tau = pgt\sin(\alpha) \qquad (1)$$

The basal shear stress below the ELA was averaged and applied to the flow line above the ELA to extrapolate the ice thickness up valley.

The shape factor is a way to systematically correlate the width versus depth of valleys. It is on a zero to one scale and is dependent upon the cross-sectional area data of the valley. The shape factor was estimated using a spreadsheet model and the basal shear stress was kept constant at 100,000kPa because it is the standard unit of measure at the ELA for a steady-state glacier. The actual basal shear stress was calculated in bars for every 500 meters until the ELA and then the model were applied to extrapolate the ice extent above the ELA.

The estimated ice extent was used in conjunction with valley topography to calculate the thickness of ice at points every 500 meters along a flow line below the ELA. This adapted model uses the last ice surface elevation before the ELA as a starting point to extrapolate the ice thickness above the ELA. The last ice surface elevation is added to the change in elevation estimated by equation (4):

$$\Delta E = (\tau L)/(tpg) \qquad (4)$$

Change in elevation (ΔE) is found by using equation (4) where, τ is basal shear stress, L is the step length, t is the ice thickness, p is ice density and g is the acceleration due to gravity. The basal shear stress below the ELA is averaged and assumed constant above the ELA. The extrapolated ice thickness of the valley above the ELA is calculated by subtracting the calculated ice surface elevation by the measured valley floor elevation (Appendix 2).

Lake Fork Canyon

The Lake Fork Canyon was interpreted by using a similar modeling technique to calculate the surface velocity, average basal shear stress, and discharge allowing for the deduction of the melting rate, total ablation zone area, and the total annual ice discharge at the ELA for the post-glaciated valley, and ultimately the interpretation of the paleoclimate.

The center flow-line was segmented every 500 meters from the terminal moraine up to the ELA. Lateral moraines were used to estimate the ice thickness up to the ELA. Every 500 meters the bedrock and moraine crest elevations were recorded and used to calculate the ice thickness through the construction of cross-sectional profiles. Equation (1) is used to calculate the basal shear stress using the ice thickness, ice density, gravity and the surface slope of the valley.

$$\tau = \mathrm{pgtsin}(\alpha)$$

The basal shear stress above the ELA is assumed to be constant and the basal slip is assumed to be zero which allows for the surface velocity to be calculated. In this equation, A is constant, 0.167 bars, τ_b is the calculated average basal shear stress in bars, H is the thickness in meters of ice and n is equated to 3 (Murray and Lock 1989).

$$V_c = 2A\tau_b{}^{n}H(n+1) \qquad (2)$$

The center flow-line velocity, equation (2) reduced by a factor of 0.63 and then multiplied by the cross-sectional area was used to calculate the minimum total discharge, Q (Murray and Locke 1989).

To derive an accurate total discharge of the Lake Fork Canyon, I needed to account for the additional inputs from adjacent valleys. The three smaller valleys fueled the flow into the Lake Fork resulting in a higher total melt water discharge (Figure 4). The cross-sectional area of each of these three smaller valleys was computed and then equation (2) was used to calculate the velocity which was then added to the other valley's discharge to deduce the total maximum ice discharge for the Lake Fork (Appendix 3).

Assuming a steady-state glacier, the velocity can be used to estimate the valley discharge and ultimately the mass balance of the glacier. The ablation zone of the Lake Fork Canyon was subdivided into five major regions (Figure 5). The area was calculated for each individual region and then multiplied by an estimated melting rate. An estimated ablation gradient is multiplied by the difference in elevation between the sections of the ablation zone (Figure 5). The melt rate ($\dot{r}$) is averaged and then multiplied by the total area for each section (Λ). The melt water multiplied by the each cross-sectional area using equation (3) is totaled and equal to the total discharge of the valley. Using trial and error the total discharge (Equation 2) needs to equal the summed melt water and cross-sectional area value in order to deduce the ablation gradient for the valley.

$$\sum_{i=1}^{n}(\dot{r} * \Lambda) \qquad (3)$$

Using equation (3) the summation of the melt water rate multiplied by each individual ablation area is equal to the maximum discharge from equation (2) and the ablation gradient can be deduced for the post-glaciated valley (Appendix 3).

Basal sliding was likely to have occurred throughout the Lake Fork even though in the model the basal sliding was assumed to be zero. To justify the ablation gradient the total discharge was increased by increments of 10%. The total discharge of the Lake Fork was multiplied by a factor of 1.10 and then the estimated ablation gradient recalculated to account for the altered discharge. This process was repeated through a 90% basal sliding error rate (Table 2). Ultimately, the size of the ablation gradient gives an approximation of the paleoclimate. This model is adapted to the Uinta Mountains and is applied to the Rhodes Canyon and Lake Fork for the last Quaternary glaciation.

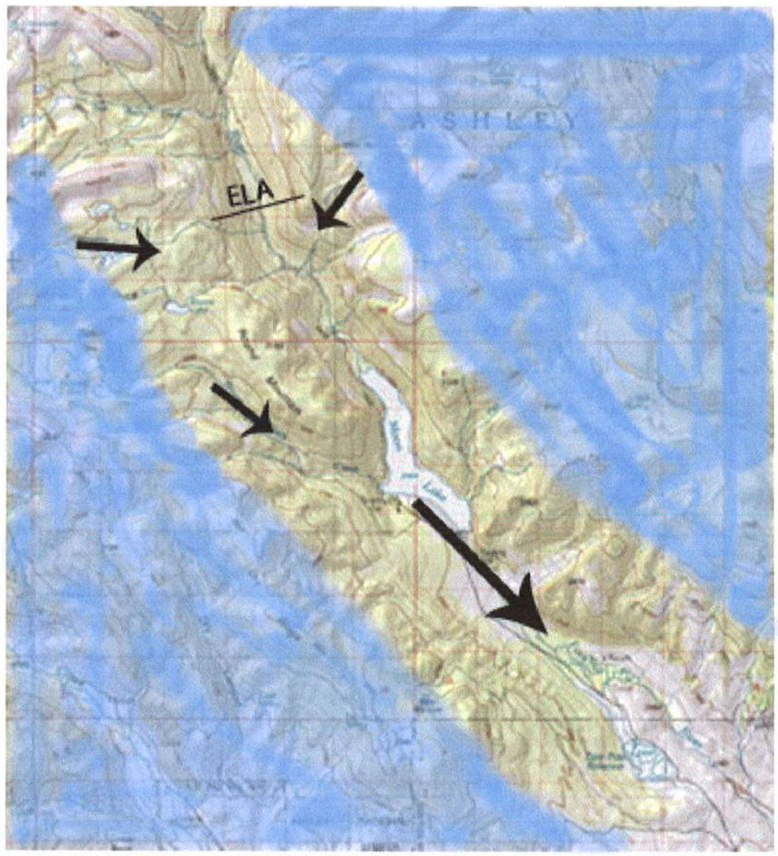

Figure 4. Topographic map of the Lake Fork. Ice is flowing in from adjacent valleys marked with small arrows. The glacial flow of the Lake Fork is marked with a larger arrow, Uinta Mountains.

RESULTS

Rhodes Canyon

Rhodes Canyon is approximately 3,500 meters from the terminal moraine to the ELA; following the center line. Above 3,500 meters, the valley forks and is fed by the Left Fork and the Mill Fork valleys (Figure 2B). The ice thickness gradually increased from the terminal moraine until the ELA where it reached a maximum height of 98 meters. The average basal shear stress below the ELA of Rhodes Canyon is 60,000kPa or 0.60 bars (Table 1). The shape factor of the valley is approximately 0.8 meaning that Rhodes Canyon has steep valley walls which reduces basal stress. Assuming the average basal shear stress below the ELA is constant for the region above the ELA and also assuming that there is a constant shape factor for the remainder of the valley, the extrapolation of ice thickness above the ELA eventually increases to a final thickness of 100 meters through the Left Fork and 156 meters above the Mill Fork. This ice thickness covers the entire upper portion of Rhodes Canyon and flows into all adjacent valleys including Soapstone Basin and Wolf Creek (Appendix 2).

Rhodes Canyon Data Table *Table (1)*

Up-Ice Distance (m)	Valley Floor Elevation (m)	Moraine Crest Elevation (m)	Measured Ice Thickness (m)	Calculated Basal Shear Stress (bars)	Calculated Surface Slope
0	2365	2365	0	0.00	0.00
500	2420	2481	61	0.88	0.16
1000	2469	2530	61	0.49	0.09
1500	2524	2573	49	0.42	0.10
2000	2560	2627	67	0.65	0.11
2500	2603	2682	79	0.55	0.09
3000	2633	2707	73	0.59	0.08
3500	2676	2774	98	0.62	0.10
				Average: 0.60	

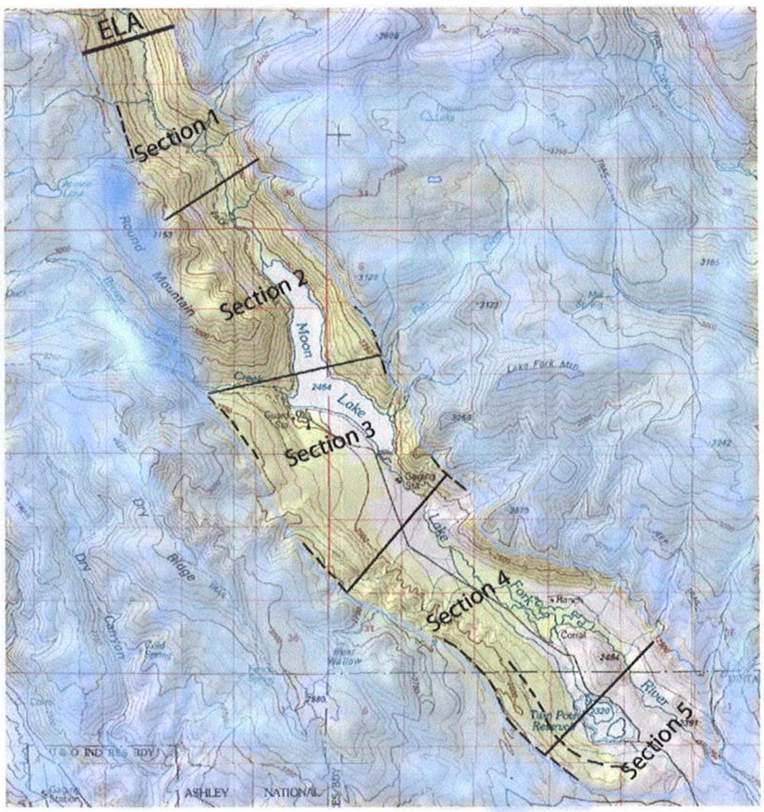

Figure 5. Shaded ablation zone of Lake Fork Canyon with measured ELA (2676m). The ablation zone was subdivided into 5 major regions and the crest of moraines are marked with dashed lines.
Section 1 area - 70,000 square km
Section 2 area - 105,000 square km
Section 3 area - 187,500 square km
Section 4 area - 81,250 square km
Section 5 area - 87,200 square km

Lake Fork Canyon

The calculated ice surface thickness at the base of Lake Fork Canyon rose to a thickness of 329 meters at the ELA. Cross sections were interpreted to deduce the basal shear stress along the flow line. The total area of the ablation zone is 530,950km^2. The annual melt rate for each segment of the ablation zone was calculated and then totaled (Figure 4). The total ablation area multiplied by the gradient gives the mass flux of the glacier (Appendix 3). The corresponding melt rate and total discharge results in an ablation gradient of 0.015mm/m for the Lake Fork Canyon. The three smaller valleys contribute to the fueling of ice flow down through the Lake Fork Canyon and have a total discharge of 198,356.81m^3/yr resulting in a total maximum ice discharge of 2,300,000 m^3/yr which in turn results in an ablation gradient minimum of 0.015mm/m and a maximum of 0.017mm/m. To account for the assumption of zero basal sliding the maximum discharge of the Lake Fork was multiplied by factors of 10% to account for all possible scenarios (Table 2). At the maximum rate of basal sliding the ablation gradient reaches a slope of 0.306mm/m. The paleoclimate can be deduced from the ablation gradient in collaboration with the melt water rate. The low gradient implies a minimal amount of melting and a small mass flux. In order for a glacier to form with little melting, it must have existed in a very cold and dry climate.

Basal Sliding % Error for Ablation Gradient *Table (2)*

Sliding Factor (%)	Total Discharge (m^2)	Ablation Gradient (mm/m)
0%	2.3E+06	0.0170
10%	2.53E+06	0.0187
20%	2.76E+06	0.0203
30%	2.98E+06	0.0220
40%	3.22E+06	0.0238
50%	3.45E+06	0.0255
60%	3.68E+06	0.0272
70%	3.91E+06	0.0289
80%	4.15E+06	0.0306
90%	4.37E+06	0.0323

DISCUSSION AND INTERPRETATION

Rhodes Canyon

The reconstruction of Rhodes Canyon's ice thickness at the top of the post-glaciated valley indicates an ice thickness of over 100 meters. This ice cap interpretation results in an increase in ice flow through Rhodes Canyon. Topographically Rhodes Canyon does not seem glaciated because of its steep, narrow side walls. The base of Rhodes Canyon is characterized by hummocky topography caused by the stagnation of ice at the base and then melting unevenly and retreating back up valley.

The highest elevation above Rhodes Canyon is 3069 meters and the maximum height of the ice thickness is between 3111 and 3119 meters meaning no part of Rhodes Canyon was unglaciated. The ice cap overlying the top of Rhodes Canyon resulted in an overflow of ice and melt water into Soapstone Basin and Wolf Creek Basin causing an increase in glacial landforms and erosion features. The ice cap had a large influence on adjacent glacial valleys by increasing the flow of ice and ultimately increasing the rate of erosion (Figure 2B).

Rhodes Canyon Ice Cap Results *Table (3)*

	Valley Floor Elevation (m)	Shape Factor	Basal Shear Stress (bars)	Calculated Ice Thickness (m)	Ice Surface Elevation (m asl)
Mill Fork	9720	0.8	60000	155.67	3118.36
Left Fork	9880	0.8	60000	99.32	3110.75

Lake Fork Canyon

The ablation gradient for the Lake Fork Canyon using glacial modeling assumes a basal sliding of zero was exceedingly small, 0.017mm/m. At the maximum basal sliding the ablation gradient was only 0.0323mm/m. Starting at the ELA there is an increase of 0.017m/mm of melting for every one meter drop in elevation. The low ablation gradient is interpreted as a steady-state glacier with no melt water flow or sliding. The lack of melt water and little basal shear stress supports the conclusion that the glacier was frigid and adhered to its bed. The paleoclimate indicated from these results show an exceptionally arid climate with a diminutive amount of precipitation.

J. Munroe researched the ablation gradients on other post-glaciated valleys on the western side of the Uinta Mountains and concluded an approximate gradient between 1 and 1.5mm/m (Munroe and Mickelson 2002). My data shows the Lake Fork gradient being significantly smaller than other valleys in the region. The Lake Fork was either an extremely cold and dry climate or the modeling technique does not accurately reconstruct the ablation gradient based on model assumptions.

In tropical regions the formation of glaciers relies heavily on high precipitation rates. An average ablation gradient for a tropical climate is about 15-18mm/m. The climate is more moderate allowing for a much higher melt water rate resulting in a steeper valley gradient. This type of climate ultimately reflects heavy amounts of precipitation on a glacier.

CONCLUSION

An ice cap covered the entirety of Rhodes Canyon and the paleoclimate of the Lake Fork was extremely cold and dry. Glacial modeling allows for the reconstruction of glaciers in hopes to bring forth new information about the processes of ice dynamics. Variations of glacial models were used on both Rhodes Canyon and Lake Fork Canyon to help interpret the formation and movement of glaciers during the Quaternary period.

The moraines are used for the extrapolation of ice extent and ice thickness up valley. According to my data, Rhodes Canyon has an ice thickness which added to the moraine crest elevation exceeds current topographic elevations resulting in the formation of an ice cap. An ice cap would increases the ice flow through adjacent valleys with lower elevations resulting in enlarged glacial features. The ice cap overlying Rhodes Canyon helps explain glacial phenomenon throughout adjacent regions.

The moraine data throughout the Lake Fork was far more extensive than Rhodes Canyon allowing for a different interpretation of glacial geology. The vast size of the valley enabled the ablation zone to be analyzed. The model results show that below the ELA of the Lake Fork there was a minimal ablation gradient, meaning there was minimal melt water flowing through the valley. The low ablation gradient suggests a very cold and dry paleoclimate for the Lake Fork. Glacial reconstruction allows for the interpretation and analysis of the ice dynamics and formation of glaciers. The more information present regarding glacial flow, the more features and formations on earth can be understood. By examining the characteristics of glacial flow for post-glaciated valleys, the exploration of paleoclimates can help pave the way for future glacial reconstructions.

REFERENCES

Benn, Douglas I., and David Evans. Glaciers and Glaciation. New York: Arnold, 1998.

Bennett, Matthew R., and Neil F. Glasser. Glacial Geology: Ice Sheets and Landforms. West Sussex, England: John Wiley and Sons, 1996.

Brugger, Keith A., and Barry S. Goldstein. "Paleoglacier reconstruction and late Pleistocene equilibrium-line altitudes, southern Sawatch Range, Colorado." Geological Socierty of America, special paper 337. (1999).

Evans, David, ed. Glacial Landsystems. London, England: Arnold, 2003.

Humphrey, Neil. "Characteristics of the Bed of the Lower Columbia Glacier, Alaska." Journal of Geophysical Research 98 (1993): 837-846.

Laabs, B.J.C. 2004. *Late Quaternary Glacial and Paleoclimate of the Southern Uinta Mountains, Utah:* [Ph.D dissertation], Uinversity of Wisconsin-Madison, 162 pp.

Laabs, B.J.C., Carlson, E.C., 2005. Glacial geology of the southern Uinta Mountains, *In*, Dehler, C.M., Peterson, J.L., Sprinkel, D.A., and Kowallis, B.J. (ed.), *Uinta Mountain Geology*: Utah Geological Association Publication 33, p. 235-253.

Munroe, J.S. and Mickelson, D.M., 2002. Last Glacial Maximum equilibrium-line altitudes and paleoclimate, northern Uintah Mountains, Utah, U.S.A.: *Journal of Glaciology*, vol. 48, no. 1, p. 257-266.

Murry, Donald R., and William W. Locke. "Dynamics of the Late Pleistocene Big Timber Glacier, Crazy Mountains, Montana, USA." Journal of Glaciology Vol. 35, No. 120 (1989).

Patterson, W.S.B. The Physics of Glaciers. 3rd ed. Woburn: Butterworth-Heinemann, 1994.